METEOROLOGICAL APPLICATIONS
Meteorol. Appl. (2014)
Published online in Wiley Online Library
(wileyonlinelibrary.com) DOI: 10.1002/met.1489

Short-term forecasting of soil temperature using artificial neural network

Hossein Tabari,[a]* P. Hosseinzadeh Talaee[b] and Patrick Willems[a,c]
[a] *Hydraulics Division, Department of Civil Engineering, KU Leuven, Belgium*
[b] *Young Researchers and Elite Club, Hamedan Branch, Islamic Azad University, Hamedan, Iran*
[c] *Department of Hydrology and Hydraulic Engineering, Vrije Universiteit Brussel, Belgium*

ABSTRACT: Soil temperature is one of the most important meteorological parameters that plays a critical role in land surface hydrological processes. In the current study, artificial neural network (ANN) models were developed and tested for 1 day ahead soil temperature forecasting at 5, 10, 20, 30, 50 and 100 cm depths. Antecedent soil temperatures plus concurrent and antecedent air temperatures were used as inputs for the ANN models. Soil and air temperature data were collected from two Iranian weather stations located in humid and arid regions for the period 2004–2005. The models' accuracies were evaluated using the Nash–Sutcliffe co-efficient of efficiency, the correlation co-efficient, the root mean square error and the mean bias error between the observed and forecasted soil temperature values. The Nash–Sutcliffe co-efficient of efficiency values >0.94 and correlation co-efficient >0.96 for all the ANN models show that the models can be applied successfully to provide accurate and reliable short-term soil temperature forecasts.

KEY WORDS daily soil temperature; soil depth; air temperature; time series forecasting; multilayer perceptron

Received 1 September 2014; Revised 27 October 2014; Accepted 10 November 2014

1. Introduction

Soil temperature and its variation at various depths are unique parameters useful in understanding both the surface energy processes and regional environmental and climate conditions (Hu and Feng, 2002). Moreover, soil temperature plays an important role in hydrological and meteorological modelling (Bilgili *et al.*, 2013), and for understanding regional eco-environmental conditions and climate change (Wu *et al.*, 2013). However, measured records of soil temperature are often not available for a given site-specific project (Lei *et al.*, 2011; Wu *et al.*, 2013).

Current techniques for detecting soil temperature, such as gamma attenuation, soil heat flux, time-domain reflectometry and ground penetration radar, are expensive, bulky and present mostly surface measurements, but do not provide profound vertical temperature profiles. Additionally, their results can be influenced significantly by the noisy environment, thus requiring complex and expensive signal processing (Jackson *et al.*, 2008). The physically based models for soil temperature estimation need specific technical skills to set up and run and their input parameters are, in general, not easily available (Plauborg, 2002).

Soil temperature regimes are controlled by a number of factors, including site climate and topography, the quantity and structure of above-ground biomass and soil physical properties (Bond-Lamberty *et al.*, 2005). For this reason, estimation and modelling of soil temperature are rather difficult, especially near the ground surface where the soil temperature variations are the highest (Mihalakakou, 2002). This has led to a number of studies to explore simple and powerful tools for such estimation and modelling. The successful application of artificial neural networks (ANNs) to model dynamic systems in areas of science and engineering suggests that the ANN approach has become one of the commonly used and powerful alternative techniques to deal with time series forecasting (Yadav *et al.*, 2011). An ANN is a non-linear mathematical structure that is capable of representing arbitrarily complex non-linear processes that relate the inputs and outputs of any system (Hsu *et al.*, 1995).

In recent years, several studies have reported that the ANN with its ability to model non-linear relationships may offer a promising alternative for soil temperature modelling. Although several applications of ANNs for this type of modelling exist (George, 2001; Mihalakakou, 2002; Bilgili, 2010; Ozturk *et al.*, 2011; Tabari *et al.*, 2011; Bilgili *et al.*, 2013; Wu *et al.*, 2013; Hosseinzadeh Talaee, 2014; Kim and Singh, 2014; Kisi *et al.*, 2014), they have so far been restricted to the research environment. The outcomes of such researches are encouraging, as the ANN method has been found to be very useful in providing important information regarding the non-linear characteristics of soil temperature and its predictability. Some of these studies used meteorological data as inputs for the ANN models (e.g., George, 2001; Mihalakakou, 2002; Bilgili, 2010; Tabari *et al.*, 2011; Hosseinzadeh Talaee, 2014). Another study by Bilgili *et al.* (2013) estimated soil temperatures of a target station using only the soil temperatures of neighbouring stations without any consideration of the other variables or parameters related to soil properties. Wu *et al.* (2013) developed ANN models for spatiotemporal interpolation of soil temperature at a depth of 10 cm in a complex terrain region with latitude, longitude, elevation, topographic wetness index and normalized difference vegetation index as inputs.

In the present research, concurrent and antecedent air temperature with time lags of 1 and 2 days, and antecedent soil temperature with lag times of 1, 2 and 3 days were used as inputs for the ANN models. Furthermore, the influence of site climate conditions on the accuracy of the soil temperature forecasts was investigated by conducting the research in different climatic regions.

* Correspondence: H. Tabari, Hydraulics Division, Department of Civil Engineering, KU Leuven, Kasteelpark Arenberg 40, BE-3001 Leuven, Belgium. E-mail: hossein.tabari@bwk.kuleuven.be or tabari.ho@gmail.com

© 2014 Royal Meteorological Society

Table 1. Performance evaluation criteria.

Evaluation criteria	Definition
Correlation co-efficient (r)	$r = \left[\dfrac{\sum_{i=1}^{n} \left(y_i^{o} - \overline{y}^{o}\right)\left(y_i^{f} - \overline{y}^{f}\right)}{\sqrt{\sum_{i=1}^{n} \left(y_i^{o} - \overline{y}^{o}\right)^2 \sum_{i=1}^{n} \left(y_i^{f} - \overline{y}^{f}\right)^2}} \right]$
Root mean square error (RMSE)	$\mathrm{RMSE} = \sqrt{\dfrac{\sum_{i=1}^{n} \left(y_i^{o} - y_i^{f}\right)^2}{n}}$
Mean bias error (MBE)	$\mathrm{MBE} = \frac{1}{n} \sum_{i=1}^{n} \left(y_i^{f} - y_i^{o}\right)$
Co-efficient of efficiency (E)	$E = 1 - \dfrac{\sum_{i-1}^{n} \left(y_i^{o} - y_i^{f}\right)^2}{\sum_{i=1}^{n} \left(y_i^{o} - \overline{y}^{o}\right)^2}$

y_i^{o} and y_i^{f} are the observed and forecasted soil temperature values at time t, respectively, and $\overline{y}^{o}$ and $\overline{y}^{f}$ are the mean of the observed and forecasted soil temperature values corresponding to n patterns.

The main objective of the present study was to predict 1 day ahead soil temperature at six depths of 5, 10, 20, 30, 50 and 100 cm using the ANN approach at humid and arid locations.

2. Methods

2.1. Multilayer perceptron

There are many types of the ANNs for various applications available in the literature, of which the multilayer perceptron (MLP) is the simplest and therefore most commonly used ANN architecture (Berberoglu *et al.*, 2000; Tabari *et al.*, 2010; Kisi *et al.*, 2012, 2013a, 2013b; Kim *et al.*, 2013; Rezaeianzadeh *et al.*, 2013, 2014; Shiri *et al.*, 2013, 2014a, 2014b; Tabari and Hosseinzadeh Talaee, 2013). The MLP consists of three layers of neurons: (1) an input layer, (2) an output layer and (3) intermediate (hidden) layer(s). Each neuron has a number of inputs (from outside the network or the previous layer) and a number of outputs (leading to the subsequent layer or out of the network). A neuron computes its output response based on the weighted sum of all its inputs according to an activation function (Dawson *et al.*, 2006). The MLP network can mathematically be represented as follows:

$$y = f\left(\sum_{i=1}^{n} \mathbf{w}_i \mathbf{p}_i + b\right) \tag{1}$$

where $\mathbf{w}_i$ represents the weight vector, $\mathbf{p}_i$ is the input vector ($i = 1, 2 \ldots n$), b is the bias, f is the activation function and y is the output. The most common activation function, and the one

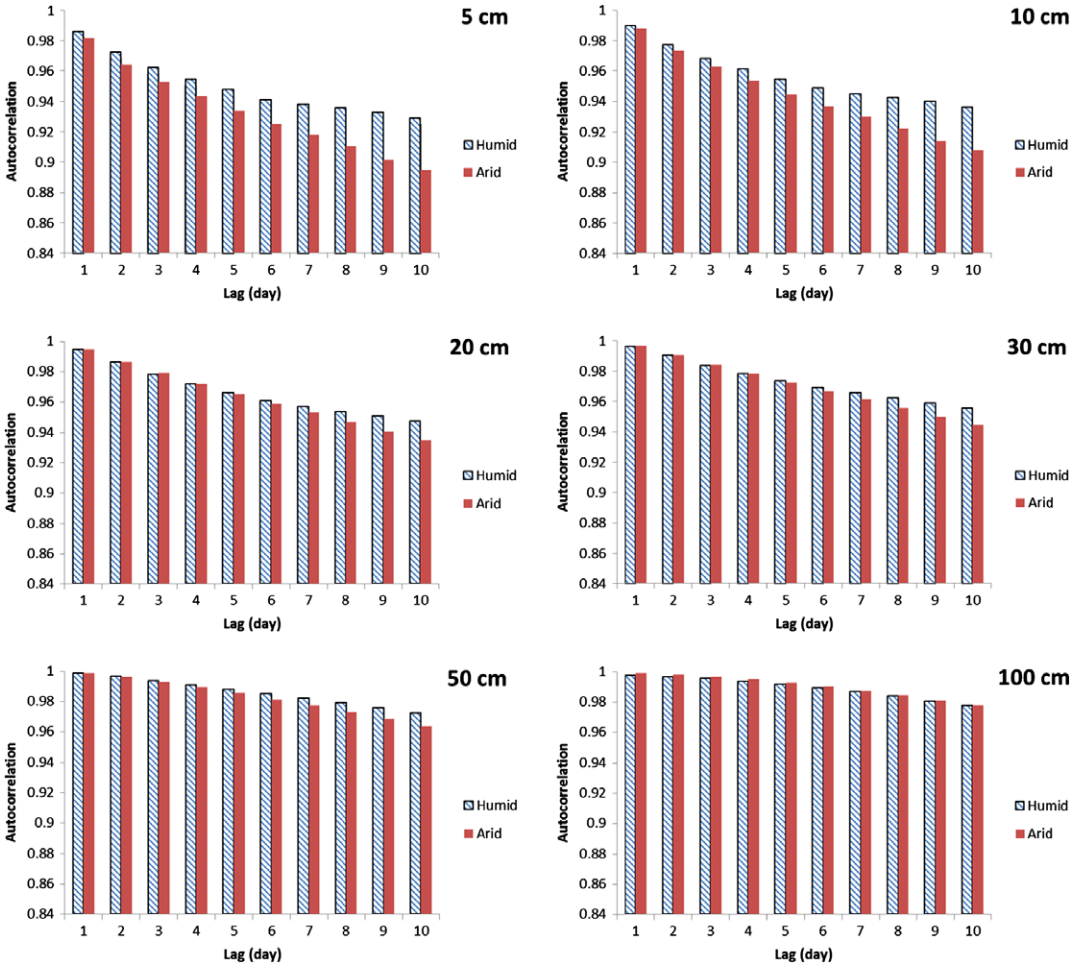

Figure 1. Autocorrelation function of soil temperature series at different depths at the study stations.

© 2014 Royal Meteorological Society

implemented in the present study, is the sigmoid function and is described as follows:

$$f(x) = \frac{1}{1 + \exp(-x)} \tag{2}$$

The characteristics of the sigmoid function are that it is bounded above and below, it is monotonically increasing and it is continuous and differentiable everywhere (Hecht-Nielsen, 1990). Sigmoid functions share a similar S-shape that is essentially linear at its centre and non-linear towards its bounds that are approached asymptotically (Yonaba *et al.*, 2010).

2.2. Levenberg–Marquardt training algorithm

Training of the ANN is the process of adjusting the weights and biases in order for the network to produce the desired output in response to every input pattern in a predetermined set of training patterns (Yonaba *et al.*, 2010). A wide range of algorithms has been developed for training the ANN to achieve the optimum model performance, while ensuring generalization and computational efficiency. The Levenberg–Marquardt (L-M) algorithm is one of the most appropriate higher order adaptive algorithms known for minimizing the mean square error (MSE) of an ANN. It is a member of a class of learning algorithms called 'pseudo second order methods'. Standard gradient descent algorithms use only the local approximation of the slope of the performance surface (error *vs* weights) to determine the best direction to move the weights for lowering the error. When the performance function has the form of a sum of squares (as is typical in training feed-forward networks), then the Hessian matrix can be approximated as:

$$\mathbf{H} = \mathbf{J}^{\mathrm{T}}\mathbf{J} \tag{3}$$

and the gradient can be determined as:

$$g = \mathbf{J}^{T}\mathbf{e} \tag{4}$$

where $\mathbf{J}$ is the Jacobian matrix that contains first derivatives of the network errors with respect to weights and biases, $\mathbf{e}$ is the vector of network errors and $\mathbf{J}^{\mathrm{T}}$ denotes the transpose of the Jacobian matrix. The Jacobian matrix can be computed through a standard back-propagation technique that is much less complex than computing the Hessian matrix.

The L-M algorithm uses this approximation to the Hessian matrix (matrix of second derivatives) in the following Newton-like update:

$$x_{k+1} = x_k - \left[\mathbf{J}^{\mathrm{T}}\mathbf{J} + \mu I\right]^{-1}\mathbf{J}^{\mathrm{T}}\mathbf{e} \tag{5}$$

When the scalar μ is zero, the L-M method becomes Newton's method, using the approximate Hessian matrix. When μ is large, the method becomes a gradient descent one with a small step size. Newton's method is faster and more accurate near an error minimum, so the aim is to shift towards Newton's method as quickly as possible. This is achieved by decreasing μ after each successful step (reduction in performance function) and increasing only when the tentative step increases the performance function. In this way, the performance function will always be reduced at any iteration of the algorithm. A key advantage of the L-M approach is that it defaults to the gradient search when the local curvature of the performance surface deviates from a parabola, which often happens in neural computing (NeuroSolutions, 2003; Kisi, 2007).

Table 2. Input vectors used for implementation of ANN models.

Model	Input vectors
I	ST ($t-1$)
II	ST ($t-1$), ST ($t-2$)
III	ST ($t-1$), ST ($t-2$), ST ($t-3$)
IV	ST ($t-1$), ST ($t-2$), ST ($t-3$), $T(t)$
V	ST ($t-1$), ST ($t-2$), ST ($t-3$), $T(t)$, $T(t-1)$
VI	ST ($t-1$), ST ($t-2$), ST ($t-3$), $T(t)$, $T(t-1)$, $T(t-2)$

ANN, artificial neural network; ST, soil temperature; T, air temperature; t, time.

Table 3. The optimum number of neurons in a hidden layer for each ANN model.

Soil depth (cm)	Model	Station		Soil depth (cm)	Model	Station	
		Zahedan	Sari			Zahedan	Sari
5	I	21	21	30	I	21	21
	II	14	14		II	14	14
	III	8	10		III	10	9
	IV	8	8		IV	8	8
	V	7	5		V	7	7
	VI	5	5		VI	6	5
10	I	21	21	50	I	21	21
	II	14	14		II	13	14
	III	10	10		III	10	10
	IV	8	9		IV	8	7
	V	7	7		V	6	7
	VI	6	7		VI	6	6
20	I	21	21	100	I	22	21
	II	14	14		II	14	15
	III	10	9		III	10	12
	IV	7	7		IV	7	9
	V	6	7		V	7	7
	VI	6	6		VI	6	5

ANN, artificial neural network.

3. Application and results

A 2 year daily data record (1 January 2004–31 December 2005) of the soil and air temperatures used in the present study was measured by the Islamic Republic of Iran Meteorological Organization (IRIMO) at two synoptic stations in Iran. The data were collected from the Sari (36 ° 33 ′ N, 53 ° 00 ′ E; 23 m a.s.l.) and Zahedan (29 ° 28 ′ N, 60 ° 53 ′ E; 1370 m a.s.l.) stations. According to the Koppen climate classification, the Sari weather station is located in a humid (Cfa: wet in all seasons) climate region in the northern part of Iran and the Zahedan station is situated in an arid (BWh: hot arid desert) climate region in the southeastern part of the country. The mean monthly temperature at Sari station varies from 9 °C in January to 28 °C in August, with an annual mean of 18 °C. At Zahedan station, mean air temperature ranges between 7 °C in January and 29 °C in July, with an annual mean of 18 °C. At Sari station, July with an average precipitation of 19 mm and October with an average precipitation of 147 mm are the driest and wettest months, respectively. The annual precipitation is 790 mm. Monthly precipitation at Zahedan station ranges between <1 mm in June and 21 mm in January, with an annual average of 90 mm. Soil temperature regimes at Rasht and Zahedan locations are thermic and hyperthermic, respectively, while soil moisture regimes at the locations are udic and aridic, respectively. The soil textures at Rasht and Zahedan locations are mainly silt clay and sandy loam, respectively.

© 2014 Royal Meteorological Society

Table 4. Performance of the ANN models for 1 day ahead soil temperature forecasting at humid Sari station.

Soil depth (cm)	Model	*r*	RMSE (°C)	MBE (°C)	*E*	Soil depth (cm)	Model	*r*	RMSE (°C)	MBE (°C)	*E*
5	I	0.974	1.879	−0.071	0.949	30	I	0.996	0.613	−0.135	0.991
	II	0.969	2.061	−0.127	0.940		II	0.997	0.549	−0.015	0.993
	III	0.974	1.919	−0.046	0.948		III	0.997	0.546	−0.068	0.993
	IV	0.987	1.435	−0.507	0.971		IV	0.998	0.416	0.009	0.996
	V	0.989	1.241	−0.293	0.978		V	0.998	0.415	0.021	0.996
	VI	0.989	1.251	−0.165	0.978		VI	0.998	0.389	−0.003	0.996
10	I	0.985	1.377	−0.068	0.969	50	I	0.998	0.311	−0.091	0.997
	II	0.985	1.363	0.053	0.969		II	0.999	0.259	−0.049	0.998
	III	0.985	1.365	−0.048	0.970		III	0.999	0.271	−0.023	0.997
	IV	0.992	1.046	−0.287	0.983		IV	0.999	0.219	0.038	0.998
	V	0.994	0.873	−0.176	0.988		V	0.999	0.211	0.026	0.998
	VI	0.995	0.836	−0.159	0.989		VI	0.999	0.204	0.017	0.999
20	I	0.994	0.779	−0.063	0.988	100	I	0.996	0.431	0.219	0.984
	II	0.995	0.719	0.039	0.989		II	0.998	0.289	0.118	0.993
	III	0.995	0.735	−0.048	0.989		III	0.998	0.283	0.088	0.993
	IV	0.998	0.512	−0.106	0.995		IV	0.998	0.299	0.149	0.993
	V	0.997	0.507	−0.057	0.995		V	0.998	0.297	0.162	0.993
	VI	0.997	0.533	−0.043	0.994		VI	0.998	0.294	0.148	0.993

ANN, artificial neural network; *r*, correlation co-efficient; RMSE, root mean square error; MBE, mean bias error; *E*, co-efficient of efficiency.

Table 5. Performance of the ANN models for 1 day ahead soil temperature forecasting at arid Zahedan station.

Soil depth (cm)	Model	*r*	RMSE (°C)	MBE (°C)	*E*	Soil depth (cm)	Model	*r*	RMSE (°C)	MBE (°C)	*E*
5	I	0.985	1.735	−0.101	0.969	30	I	0.994	0.985	−0.229	0.987
	II	0.985	1.753	−0.156	0.969		II	0.996	0.830	0.006	0.991
	III	0.986	1.659	−0.183	0.972		III	0.995	0.921	−0.148	0.989
	IV	0.990	1.405	−0.119	0.980		IV	0.998	0.621	0.007	0.995
	V	0.990	1.387	−0.146	0.981		V	0.997	0.663	−0.019	0.994
	VI	0.991	1.356	−0.121	0.981		VI	0.997	0.669	−0.026	0.994
10	I	0.988	1.498	−0.131	0.975	50	I	0.997	0.648	0.017	0.992
	II	0.989	1.438	−0.103	0.977		II	0.997	0.589	0.050	0.994
	III	0.988	1.459	−0.095	0.976		III	0.996	0.677	−0.009	0.992
	IV	0.994	1.092	−0.206	0.987		IV	0.996	0.665	0.024	0.992
	V	0.994	1.088	−0.159	0.987		V	0.998	0.550	0.100	0.995
	VI	0.994	1.056	−0.174	0.988		VI	0.997	0.557	−0.004	0.994
20	I	0.993	1.087	−0.279	0.986	100	I	0.979	1.208	0.431	0.938
	II	0.995	0.976	−0.004	0.989		II	0.977	1.213	0.418	0.934
	III	0.993	1.073	−0.070	0.986		III	0.979	1.182	0.450	0.942
	IV	0.997	0.735	−0.100	0.993		IV	0.977	1.207	0.510	0.939
	V	0.997	0.743	−0.128	0.993		V	0.977	1.209	0.521	0.939
	VI	0.997	0.701	−0.172	0.994		VI	0.981	1.166	0.523	0.944

ANN, artificial neural network; *r*, correlation co-efficient; RMSE, root mean square error; MBE, mean bias error; *E*, co-efficient of efficiency.

Soil temperatures at depths of 5, 10, 20, 30, 50 and 100 cm were measured by mercury-in-glass thermometers (accuracy of ±0.2 °C) read by the observer. For soil temperature measurements at shallow layer (i.e. 5, 10, 20 and 30 cm depths), the thermometer with its stem bent at a right angle is placed into the ground and does not need to be removed for readings. For soil temperature measurements at 50 and 100 cm, straight thermometers are placed underground. These thermometers are removed and replaced for each observation.

For a given depth/station, the data were divided into different groups: training data set, cross-validation data set and testing data set. The first 60% of the data (438 daily values starting from 1 January 2004) were used for training, the following 15% of the data (112 daily values) were for cross-validation and the rest (181 daily values) were testing data. Once the available data have been divided into their subsets (i.e. training, cross-validation and validation), it is important to pre-process the data in a suitable form before they are applied to the ANN (Shahin *et al.*, 2008). Data pre-processing is necessary to ensure all variables receive equal attention during the training process (Maier and Dandy, 2000). Moreover, pre-processing usually speeds up the learning process. Pre-processing can be in the form of data scaling, normalization and transformation (Masters, 1993).

Because of the use of sigmoid functions in the ANN model, the data must be normalized into the range [0, 1] before applying the ANN methodology. It was found to be useful to normalize the time series to the range [0.05, 0.95] to avoid the problem of output signal saturation that can sometimes be encountered in ANN applications (Smith, 1993). Thus, the data were normalized within the range 0.05–0.95 as follows:

$$X_n = 0.05 + 0.9\frac{X_o - X_{min}}{X_{max} - X_{min}} \quad (6)$$

where X_n and X_o are the normalized and the original inputs at a given depth/station, and X_{min} and X_{max} are the minimum and maximum of input ranges at a given depth/station, respectively.

© 2014 Royal Meteorological Society

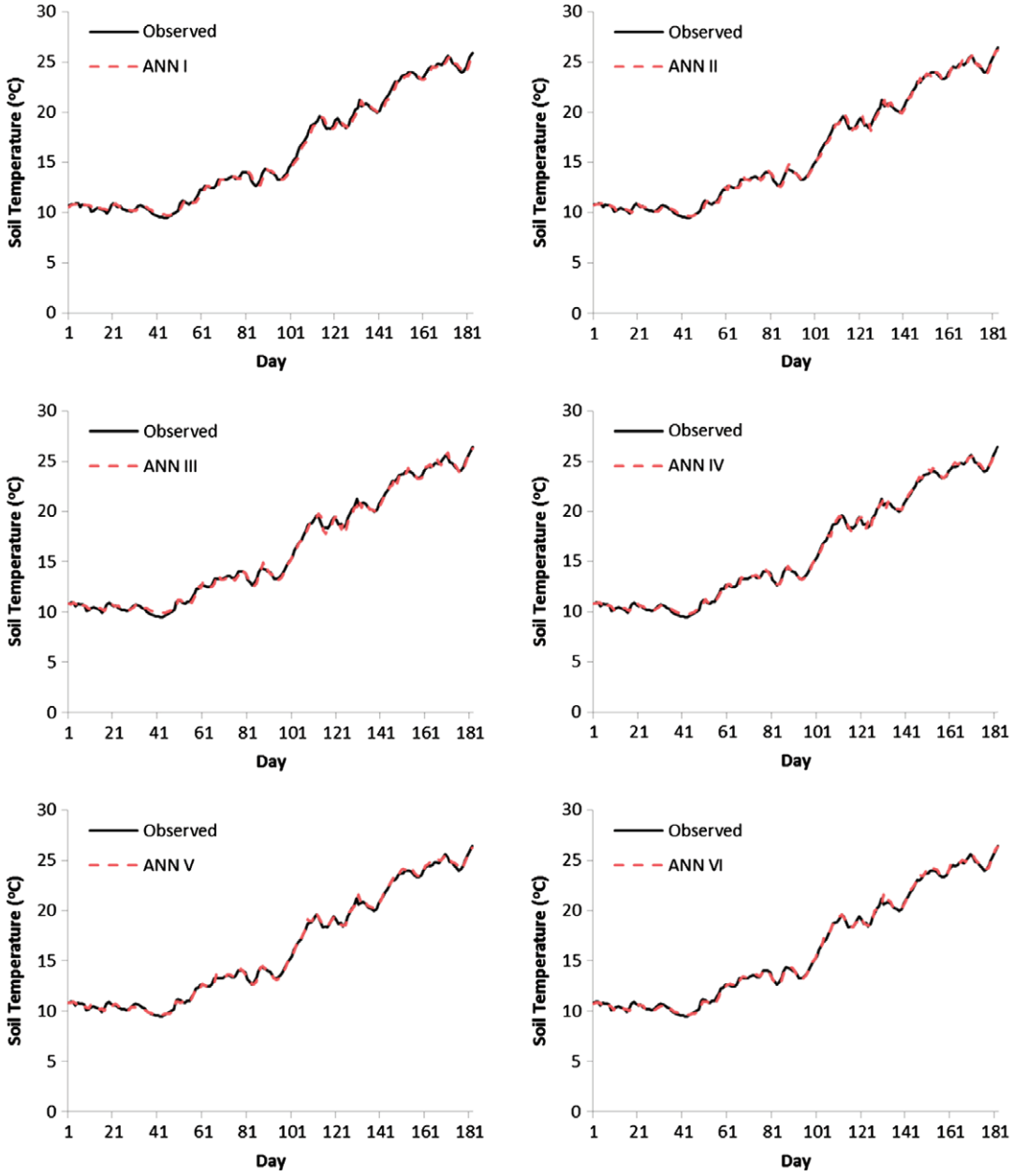

Figure 2. Time series comparison of the observed and artificial neural network (ANN) forecasted daily soil temperature series at 50 cm depth in the testing period at humid Sari station.

Once the ANN models have been successfully executed, model outputs in the form of normalized values are converted to soil temperatures by inverse transformation.

The performances of the ANN models were evaluated using the root mean square error (RMSE), the mean bias error (MBE), the co-efficient of efficiency (Nash and Sutcliffe, 1970) and the correlation co-efficient (r) between the observed and forecasted values. The definition of these evaluation criteria is provided in Table 1.

The autocorrelation of the whole dataset time series was analysed for evaluating the effects of antecedent soil temperatures at different depths. The autocorrelation statistics for lag 1 to lag 10 for soil temperatures at different depths at the study stations are shown in Figure 1. As shown, the autocorrelation co-efficients at the considered lags are high and statistically significant for all soil depths considered. The gradually decaying pattern of the autocorrelation function confirms the dominance of the autoregressive process. A closer look at the autocorrelation co-efficients for different depths indicates a stronger memory of the soil temperature time series in the deeper soils than that in the shallower ones. As can be seen from Figure 1, at the humid location, the soil temperature at 50 cm depth has the highest autocorrelation co-efficient at lag 1, and thereafter (from lag 2 to lag 10) the soil temperature at 100 cm depth shows the highest autocorrelation. At the arid location, the presence of a dominant autoregressive process is more obvious at 100 cm depth compared with other depths. These autocorrelations as a signal of high persistence are beneficial for the development of simple ANN models.

The input combinations of the ANN models tried in this work are presented in Table 2. Because the present study aimed to develop simple ANN models for soil temperature forecasting,

© 2014 Royal Meteorological Society

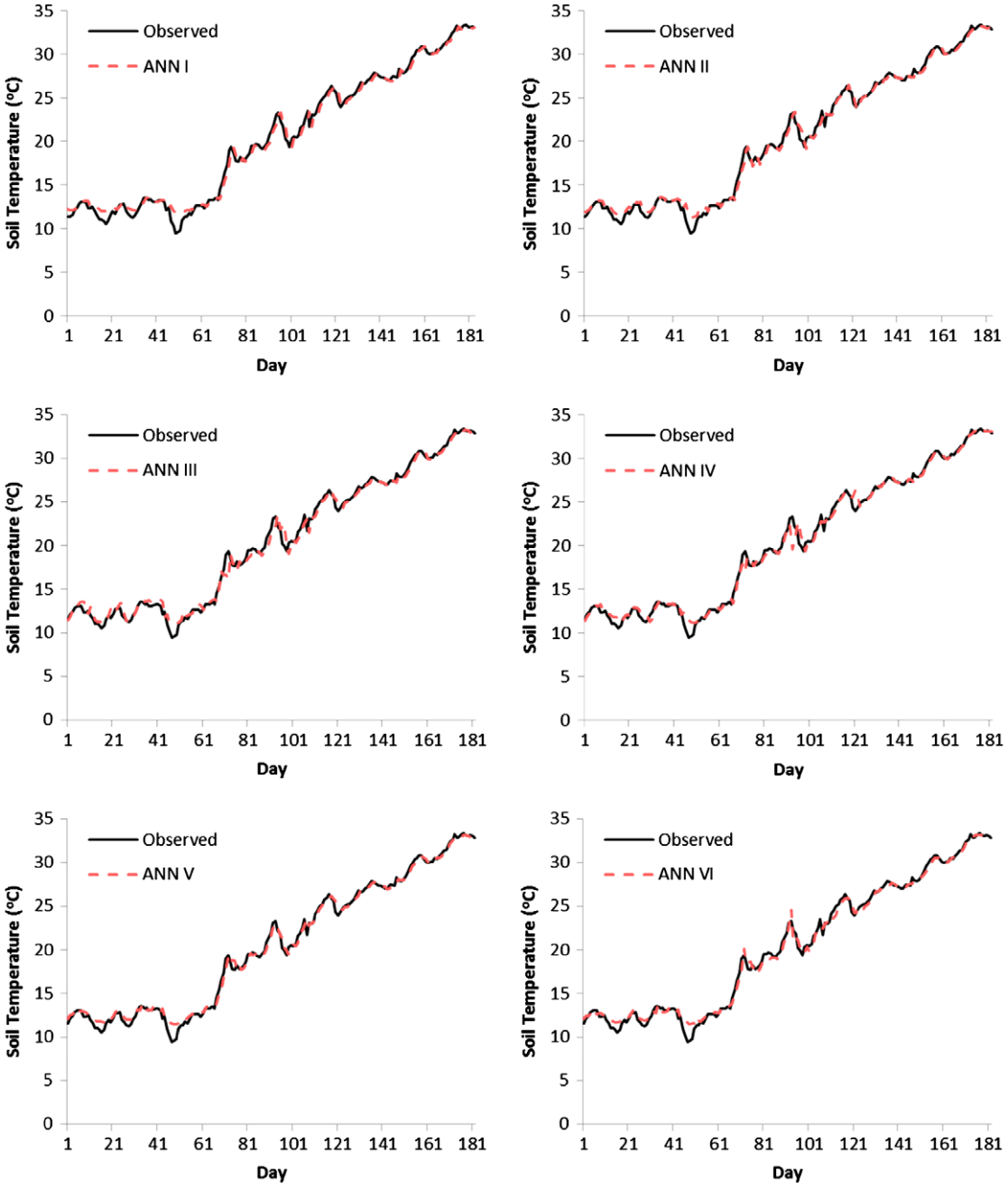

Figure 3. Time series comparison of the observed and artificial neural network (ANN) forecasted daily soil temperature series at 50 cm depth in the testing period at arid Zahedan station.

in addition to antecedent soil temperatures, only air temperature as the most effective variable for soil temperature (Tabari *et al.*, 2011; Hosseinzadeh Talaee, 2014) was added to the input vector of the ANN models. As shown in Table 2, six input combinations were evaluated for the ANN models, of which the first three combinations are based on antecedent soil temperatures and the rest are based on antecedent soil temperatures plus concurrent and antecedent air temperatures.

One of the important issues in the training of an ANN is to avoid overfitting, as it reduces its capacity for generalization. If too many neurons are included in the network, it will have too many parameters and may overfit the data. In contrast, if too few neurons are used, the network might not be able to detect the signal and variance of a complex data set fully (Kisi, 2008). Therefore, in this work, different values were considered for the number of neurons in the hidden layer. The optimum number of neurons was determined *via* a trial and error process in which the training of the ANN starts with a small number of neurons and then additional neurons are gradually added to obtain the lowest forecasting errors. The optimal number of neurons in the hidden layer for each input combination is presented in Table 3. The best way to avoid overfitting is to use plenty of training data. For noise-free data, if at least five times as many training cases as there are weights in the network are included, overfitting is unlikely (Kisi, 2008). For the most complex ANN model in this work (model VI for 10 cm soil depth at Sari station) with 6 inputs, 7 hidden and 1 output nodes, 49 weights ($6 \times 7 + 7 = 49$) were used. In the present study, 438 daily soil temperature values

© 2014 Royal Meteorological Society

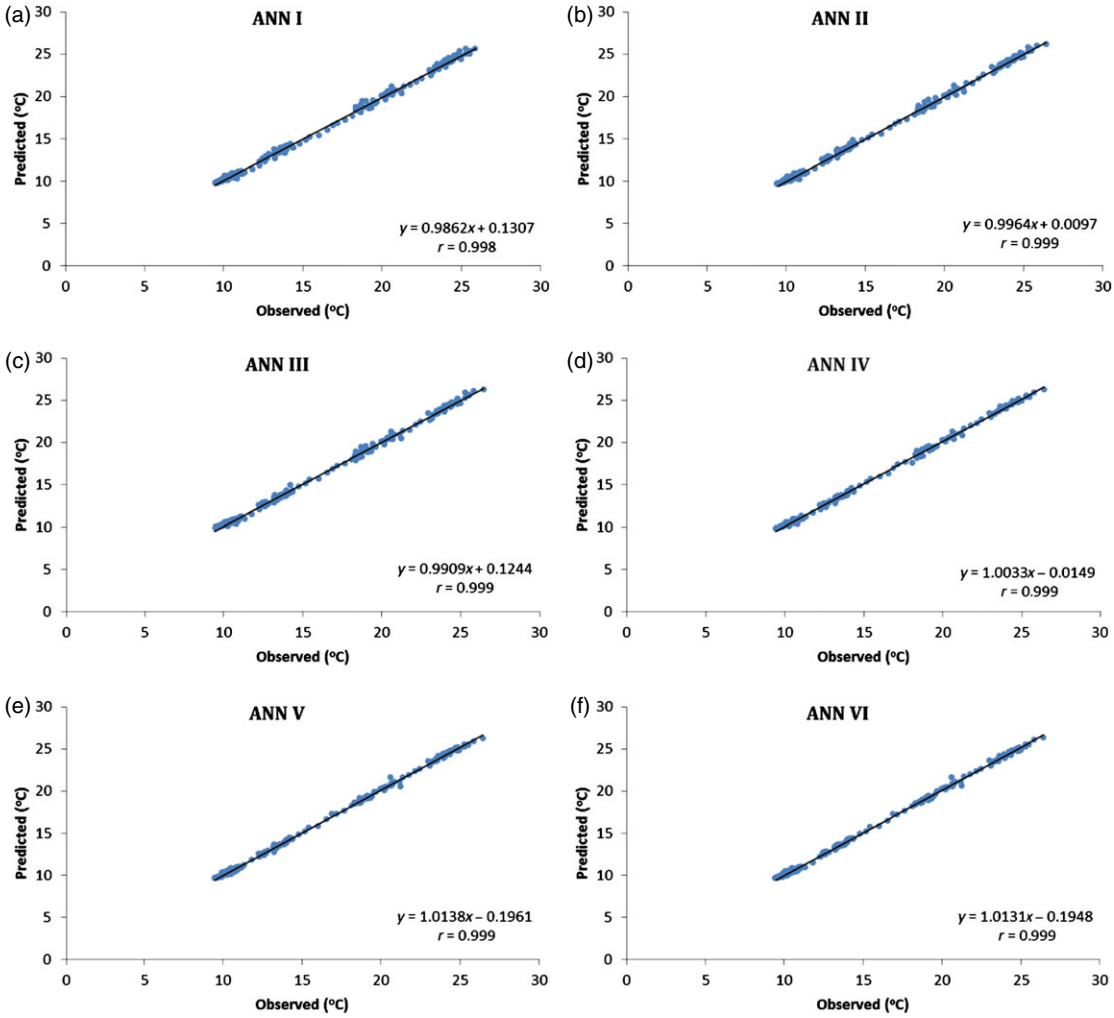

Figure 4. Scatter plot of the observed and artificial neural network (ANN) forecasted daily soil temperature series at 50 cm depth in the testing period at humid Sari station.

were used for training of the ANN models that can be considered sufficient to avoid overfitting, according to Kisi (2008). However, Wang *et al.* (2005) showed that even when the ratio of the number of training data sets to the number of weights in the network is as high as 50, a very slight overfitting can still be observed in some cases. Thus, in the present study, 15% of the data were considered as cross-validation data to avoid overtraining of the ANN by monitoring the validation error during the training process.

The performance evaluation criteria of the ANN models for 1 day ahead soil temperature forecasting at different depths are given in Tables 4 and 5. As shown, the Nash–Sutcliffe co-efficient of efficiency of all the ANN models for both stations are higher than 0.94, indicating the high efficiency of the models for 1 day ahead soil temperature forecasting. According to Shamseldin (1997), a co-efficient of efficiency ≥ 0.9 is generally considered very satisfactory. In addition, there is a strong correlation ($r > 0.96$) between the forecasted and observed soil temperature values in all the cases. From the soil surface to the depth of 30 cm, all ANN models underestimated soil temperature values. Below that depth, they overestimated the values. In both stations, the ANN model VI performed best at most of the soil depths. Generally, the performance level of the ANN models increased with the increase of the soil depth.

The inclusion of air temperature improved the results, especially in the shallower soils, which are more influenced by meteorological changes. It should be noted that at the depth of 100 cm, adding air temperature to the inputs of the ANN models (from model III to models IV and V) deteriorated the performances. When additional antecedent air temperature data were added to the input, the performance of the network improved. As there is a time lag of more than 2 days between air temperature and soil temperature at 100 cm depth, use of air temperature data from the preceding several days is recommended for soil temperature forecasting in the deeper soil layers. As shown in Tables 4 and 5, air temperature with a greater time lag is needed for soil temperature forecasting at 100 cm depth at the humid location than at the arid location.

At 5 cm soil depth, the ANN model V had the best performance ($r = 0.989$, RMSE = 1.241 °C, MBE = −0.293 °C and $E = 0.978$) at the humid location, while the ANN model VI yielded the most accurate soil temperature forecasts at the arid location ($r = 0.991$, RMSE = 1.356 °C, MBE = −0.121 °C and $E = 0.981$). This indicates that only the concurrent and the previous day air temperatures are effective for soil temperature forecasting at 5 cm soil depth at the humid location, whereas the air temperature with 2 day time lag slightly improved the performance of the ANN models at the arid location. In other words, inclusion of the concurrent air temperature to the inputs for the ANN had the

© 2014 Royal Meteorological Society

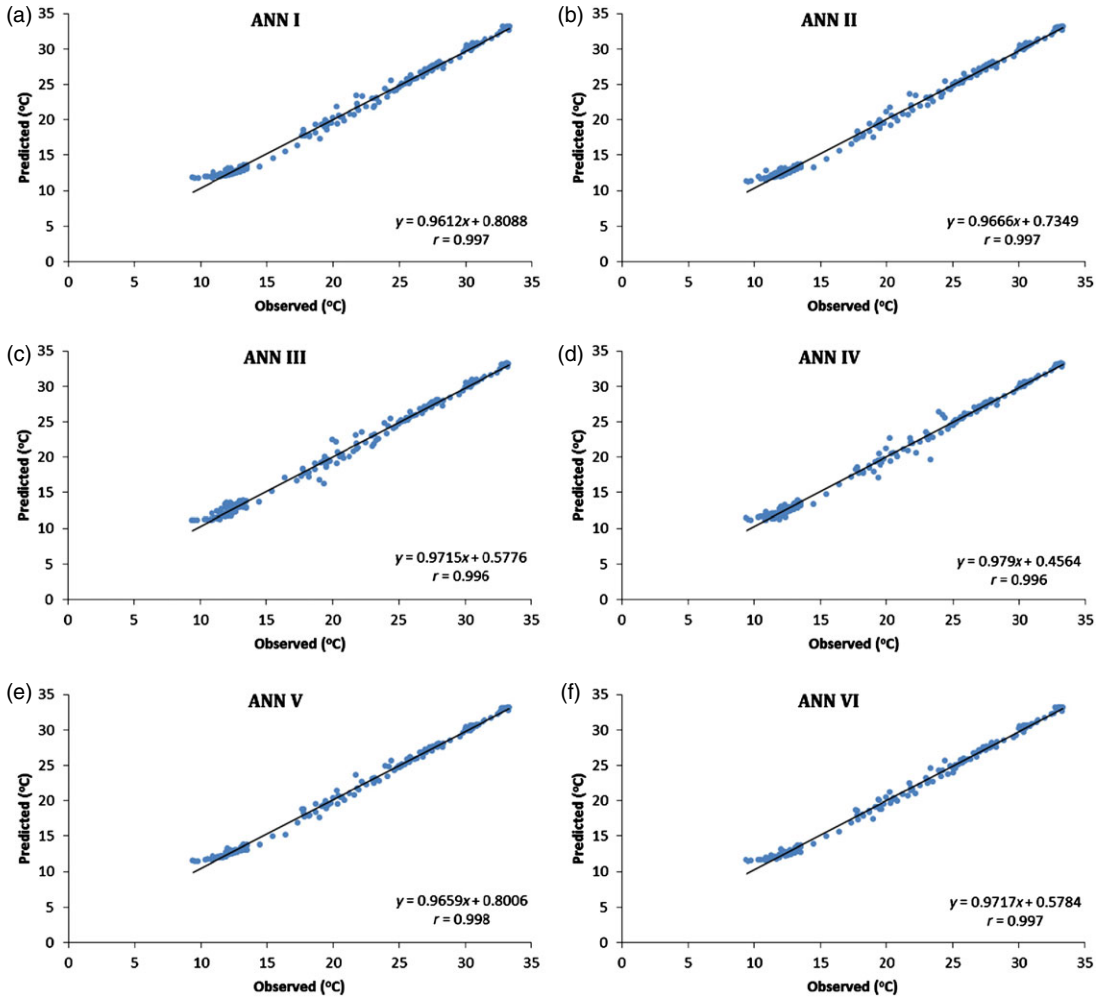

Figure 5. Scatter plot of the observed and artificial neural network (ANN) forecasted daily soil temperature series at 50 cm depth in the testing period at arid Zahedan station.

strongest effect on the results of soil temperature forecasts at 5 cm depth at the humid location. The Nash–Sutcliffe co-efficient of efficiency increased from 0.948 in the ANN model II to 0.971 in the ANN model III. When the concurrent air temperature was included in the input pattern, the forecasting error at 5 cm soil depth at the humid location decreased by 0.5 °C (from 1.919 to 1.435 °C).

The performance of ANN models for 1 day ahead soil temperature forecasting at 50 cm depth in the testing period is demonstrated in the time series of Figures 2 and 3. It is obvious from the hydrographs that the ANN models' forecasts closely follow the corresponding observed values. A closer look at the two time series (i.e. observed and forecasted) for Sari station (Figure 2) reveals that the ANN not only very well captures the major trends in the soil temperature series but also reasonably preserves the minor fluctuations. As can be seen, even extreme values are very well forecasted and the forecasted values are much closer to and almost indistinguishable from the observed values. The good agreement between the observed and forecasted series can also be revealed by plotting the scatter diagrams, as shown in Figures 4 and 5. As seen from the scatterplots, the ANN models' performances are accurate and good, where all data points are quite near the line of agreement.

The unitless Nash–Sutcliffe co-efficient of efficiency allows for a true comparison of the accuracy of the ANN models in the two climatic regions. Use of the RMSE measure for this purpose may lead to misunderstanding of the results, since the higher RMSE values of the arid location compared with that of the humid location may be due to the higher soil temperature values in the former climate. The comparison of the models' performances at the studied stations indicates that the efficiency of most of the ANN models for soil temperature forecasting at 5 and 10 cm depths at the arid location was higher than that at the humid location, although the difference was not large. For the other soil depths, the ANN models showed better performances at the humid location.

4. Discussion and conclusions

The development of artificial neural network (ANN)-based soil temperature forecasting aids for a humid and an arid synoptic station has been outlined. Six input vectors were employed for the ANN based on antecedent soil temperatures, and concurrent and antecedent air temperatures. Daily soil temperatures were recorded at six depths of 5, 10, 20, 30, 50 and 100 cm at two synoptic stations in Iran. The results indicated that all of the developed ANN models exhibited good forecasting ability. The soil temperature time series showed a statistically significant autocorrelation at all soil depths considered, indicating that the time series have high predictability, and their future values can be

© 2014 Royal Meteorological Society

forecasted very well from the past values. Furthermore, soil temperatures at the deeper layers, which are more effectively insulated by overlying soil material and are less influenced by variable surface conditions (Braley and Zarling, 1991; Schaetzl and Tomczak, 2001), revealed a stronger autocorrelation compared with the shallower soils. At the humid location, the presence of moisture at the deep soil layer disturbed the serial structure of the soil temperature time series and led to lower autocorrelation co-efficient at 100 cm depth in comparison with the arid location.

The performance level of the ANN models generally increased with the increase of the soil depth. This is due to the stronger memory of the soil temperature time series in the deeper soil layers, which increases its predictability. As the soil temperature at the deeper horizons is less influenced by short-term changes in surface meteorological conditions, its diurnal fluctuation is lower. In such situations, the observed soil temperature values at these depths are generally smooth and easier to forecast. Furthermore, inclusion of air temperature to the inputs of the ANN models increases the network's efficiency, particularly for the shallower soils. For deeper soils, use of air temperature with a time lag of more than 2 days leads to an improved forecasting performance. Owing to the higher predictability of the soil temperature time series (i.e. stronger autocorrelation) at the humid location, the forecasts for this location are generally better than those obtained at the arid location. Overall, the ANN models developed here for 1 day ahead soil temperature forecasting showed encouraging results. The results suggest that this method could provide a useful tool for solving similar types of problems in soil science and hydrology.

In the present study, short-term (1 day ahead) soil temperature forecasting was done at six soil depths for two synoptic stations. Further study is needed to test the developed ANN models at different locations. Moreover, it would be useful to test long-term forecasting of soil temperature based on previous measured series as well.

Acknowledgements

The authors are grateful to the Islamic Republic of Iran Meteorological Organization (IRIMO) for providing the data. The authors thank both the reviewers for their insightful comments on the paper.

References

Berberoglu S, Lloyd CD, Atkinson PM, Curran PJ. 2000. The integration of spectral and textural information using neural networks for land cover mapping in the Mediterranean. *Comput. Geosci*. **26**: 385–396.

Bilgili M. 2010. Prediction of soil temperature using regression and artificial neural network models. *Meteorol. Atmos. Phys.* **110**: 59–70.

Bilgili M, Sahin B, Sangun L. 2013. Estimating soil temperature using neighboring station data via multi-nonlinear regression and artificial neural network models. *Environ. Monit. Assess.* **185**: 347–358.

Bond-Lamberty B, Wang C, Gower ST. 2005. Spatiotemporal measurement and modeling of stand-level boreal forest soil temperatures. *Agric. For. Meteorol.* **131**: 27–40.

Braley WA, Zarling JP. 1991. MUT1D: user-friendly one-dimensional thermal model. In *Cold Regions Engineering*, US Army Cold Regions Research and Engineering Laboratory, Hanover, NH, Sodhi DC (ed), American Society of Civil Engineers: New York, NY; 1–10.

Dawson CW, Abrahart RJ, Shamseldin AY, Wilby RL. 2006. Flood estimation at ungauged sites using artificial neural networks. *J. Hydrol.* **319**: 391–409.

George RK. 2001. Prediction of soil temperature by using artificial neural networks algorithms. *Nonlinear Anal*. **47**: 1737–1748.

Hecht-Nielsen R. 1990. *Neurocomputing*. Addison-Wesley: Reading, MA.

Hosseinzadeh Talaee P. 2014. Daily soil temperature modeling using neuro-fuzzy approach. *Theor. Appl. Climatol.* **118**: 481–489, DOI: 10.1007/s00704-013-1084-9.

Hsu KL, Gupta HV, Sorooshian S. 1995. Artificial neural network modeling of the rainfall runoff process. *Water Resour. Res.* **31**(10): 2517–2530.

Hu QS, Feng S. 2002. *A Daily Soil Temperature Dataset and Soil Temperature Climatology of the Contiguous United States*. Climate and Bio-Atmospheric Sciences Group, School of Natural Resource Sciences, University of Nebraska-Lincoln: Lincoln, NE.

Jackson T, Mansfield K, Saafi M, Colman T, Romine P. 2008. Measuring soil temperature and moisture using wireless MEMS sensors. *Measurement* **41**: 381–390.

Kim S, Shiri J, Kisi O, Singh VP. 2013. Estimating daily pan evaporation using different data-driven methods and lag-time patterns. *Water Resour. Manage.* **27**: 2267–2286.

Kim S, Singh VP. 2014. Modeling daily soil temperature using data-driven models and spatial distribution. *Theor. Appl. Climatol.* **118**: 465–479, DOI: 10.1007/s00704-013-1065-z.

Kisi O. 2007. Streamflow forecasting using different artificial neural network algorithms. *J. Hydrol. Eng.* **12**(5): 532–539.

Kisi O. 2008. Stream flow forecasting using neuro-wavelet technique. *Hydrol. Processes* **22**: 4142–4152.

Kisi O, Kim S, Shiri J. 2013a. Estimation of dew point temperature using neuro-fuzzy and neural network techniques. *Theor. Appl. Climatol.* **114**: 365–373.

Kisi O, Shiri J, Nikoofar B. 2012. Forecasting daily lake levels using artificial intelligence approaches. *Comput. Geosci.* **41**: 169–180.

Kisi O, Shiri J, Tombul M. 2013b. Modeling rainfall-runoff process using soft computing techniques. *Comput. Geosci.* **51**: 108–117.

Kisi O, Tombul M, Kermani MZ. 2014. Modeling soil temperatures at different depths by using three different neural computing techniques. *Theor. Appl. Climatol.*, DOI: 10.1007/s00704-014-1232-x.

Lei S, Daniels JL, Bian Z, Wainaina N. 2011. Improved soil temperature modeling. *Environ. Earth Sci.* **62**(6): 1123–1130.

Maier HR, Dandy GC. 2000. Neural networks for the prediction and forecasting of water resources variables: a review of modeling issues and applications. *Environ. Model. Software* **15**: 101–124.

Masters T. 1993. *Practical Neural Network Recipes in C++*. Academic Press: San Diego, CA.

Mihalakakou G. 2002. On estimating soil surface temperature profiles. *Energy Build.* **34**: 251–259.

Nash JE, Sutcliffe JV. 1970. River flow forecasting through conceptual models: 1. A discussion of principles. *J. Hydrol.* **10**: 282–290.

NeuroSolutions. 2003. *The Neural Network Simulation Environment*. NeuroDimension Inc: Gainesville, FL.

Ozturk M, Salman O, Koc M. 2011. Artificial neural network model for estimating the soil temperature. *Can. J. Soil Sci.* **91**: 551–562.

Plauborg F. 2002. Simple model for 10 cm soil temperature in different soils with short grass. *Eur. J. Agron.* **17**: 173–179.

Rezaeianzadeh M, Stein A, Tabari H, Abghari H, Jalalkamali N, Zia Hosseinipour E, *et al.* 2013. Comparative assessment of a conceptual hydrological model and artificial neural networks for daily outflows forecasting. *Int. J. Environ. Sci. Technol.* **10**(16): 1181–1192.

Rezaeianzadeh M, Tabari H, Arabi Yazdi A, Isik S, Kalin L. 2014. Flood flow forecasting using ANN, ANFIS and regression models. *Neural Comput. Appl.* **25**: 25–37.

Schaetzl RJ, Tomczak DM. 2001. Wintertime temperature in the fine-textured soils of the Saginaw valley, Michigan. *Great Lakes Geogr.* **8**: 87–98.

Shahin MA, Jaksa MB, Maier HR. 2008. State of the art of artificial neural networks in geotechnical engineering. *Electr. J. Geotech. Eng.* **8**: 1–26.

Shamseldin AY. 1997. Application of a neural network technique to rainfall-runoff modelling. *J. Hydrol.* **199**: 272–294.

Shiri J, Kim S, Kisi O. 2014a. Estimation of daily dew point temperature using genetic programming and neural networks approaches. *Hydrol. Res.* **45**(2): 165–181.

Shiri J, Marti P, Nazemi AH, Sadraddini AA, Kisi O, Lenderas G, *et al.* 2013. Local vs. external training of neuro-fuzzy and neural networks models for estimating reference evapotranspiration assessed through k-fold testing. *Hydrol. Res.*, DOI: 10.2166/nh.2013.112.

Shiri J, Nazemi AH, Sadraddini AA, Landeras G, Kisi K, Fakheri Fard A, *et al.* 2014b. Comparison of heuristic and empirical approaches for estimating reference evapotranspiration from limited inputs in Iran. *Comput. Electron. Agric.* **108**: 230–241.

Smith M. 1993. *Neural Networks for Statistical Modeling*. John Wiley & Sons, Inc: New York, NY.

© 2014 Royal Meteorological Society

Tabari H, Hosseinzadeh Talaee P. 2013. Multilayer perceptron for reference evapotranspiration estimation in a semiarid region. *Neural Comput. Appl.* **23**(2): 341–348.

Tabari H, Marofi S, Sabziparvar AA. 2010. Estimation of daily pan evaporation using artificial neural network and multivariate non-linear regression. *Irrig. Sci.* **28**: 399–406.

Tabari H, Sabziparvar AA, Ahmadi M. 2011. Comparison of artificial neural network and multivariate linear regression methods for estimation of daily soil temperature in an arid region. *Meteorol. Atmos. Phys.* **110**: 135–142.

Wang W, Van Gelder PHAJM, Vrijling JK. 2005. Some issues about the generalization of neural networks for time series prediction. *ICANN'05 Proceedings of the 15th international conference on Artificial neural networks: formal models and their applications* – Volume Part II; 559–564.

Wu W, Tang X-P, Guo N-J, Yang C, Liu H-B, Shang Y-F. 2013. Spatiotemporal modeling of monthly soil temperature using artificial neural networks. *Theor. Appl. Climatol.* **113**: 481–494.

Yadav D, Naresh R, Sharma V. 2011. Stream flow forecasting using Levenberg-Marquardt algorithm approach. *Int. J. Water Resour. Environ. Eng.* **3**(1): 30–40.

Yonaba H, Anctil F, Fortin V. 2010. Comparing sigmoid transfer functions for neural network multistep ahead streamflow forecasting. *J. Hydrol. Eng.* **15**(4): 275–283.

© 2014 Royal Meteorological Society